CIENTIFIC Publishing Limited

New Energy Exploitation and Application
https://ojs.ukscip.com/index.php/neea

Review

Exergy-Based Performance Evaluation of Solar Dryers: A Critical Review of Adopted Approaches

Gustavo Aragão Correia , Keyse Santos Andrade , Marcos Fábio Farias Souza and Manoel Marcelo do Prado *

Department of Chemical Engineering, Federal University of Sergipe, São Cristóvão 49100-000, Brazil
* Correspondence: manoelprado@academico.ufs.br

Received: 12 March 2026; **Revised:** 8 May 2026; **Accepted:** 20 May 2026; **Published:** 14 July 2026

Abstract: Drying is a key unit operation in industrial processes, yet it is inherently energy-intensive, particularly when conventional technologies are employed. Solar dryers have emerged as sustainable alternatives due to their reduced dependence on fossil fuels and lower environmental impact. However, improving their performance requires a rigorous thermodynamic assessment, for which exergy analysis provides a more comprehensive framework by accounting for both energy quality and process irreversibilities. Despite its potential, the application of exergy analysis to solar drying systems remains inconsistent in the literature, with significant variations in definitions, assumptions, and formulations adopted. This lack of standardization compromises the reliability and comparability of reported performance indicators. In this study, the formulations commonly used in the exergy analysis of solar dryers are systematically reviewed and critically evaluated. The results indicate that the widespread use of outlet air exergy in the calculation of exergy efficiency may not adequately represent the useful energy associated with the drying process. A more physically consistent approach is obtained by considering useful energy in terms of sensible and latent heat transfer, as well as by incorporating formulations derived from radiation theory that account for material absorptance and transmittance. Furthermore, practical recommendations are proposed to improve the accuracy of exergy-based evaluations, including continuous monitoring of product temperature and mass, and modeling the drying agent as a mixture of dry air and water vapor. These findings contribute to the development of a more consistent framework for the thermodynamic assessment and comparison of solar drying systems.

Keywords: Drying; Performance Parameters; Hybrid Dryers; Exergy

1. Introduction

Drying is a fundamental unit operation in industrial and agricultural systems, playing a critical role in both product preservation and energy applications. In particular, the use of dried biomass is essential for thermochemical conversion processes, where reduced moisture content enhances fuel quality and overall process efficiency [1]. Biomass drying is also relevant for biochemical pathways, such as bioethanol production via fermentation [2]. Furthermore, moisture removal is a key factor in extending shelf life by limiting microbial activity and degradation mechanisms [3].

Despite its importance, drying is one of the most energy-intensive operations across industrial sectors. In the food industry alone, it accounts for approximately 25% of total energy consumption [4]. Conventional drying technologies, including microwave, fluidized bed, freeze, and infrared systems, contribute significantly to this high demand [5]. Given the continued reliance of the global energy matrix on fossil fuels, such demand translates into significant environmental burdens, particularly in terms of greenhouse gas emissions [4].

In this context, solar drying technologies have emerged as promising alternatives due to their potential to utilize renewable energy. These systems are particularly attractive for decentralized applications and remote regions with limited access to electricity [6]. In addition to their sustainability advantages, solar dryers exhibit considerable design flexibility, encompassing configurations such as greenhouse, direct, indirect, mixed-mode, and hybrid systems [7–9]. Depending on the design, solar dryers may operate with forced (active) or natural (passive) airflow.

Hybrid solar dryers offer enhanced operational reliability and flexibility by incorporating supplementary energy sources such as electric heaters, biomass combustion systems, liquefied petroleum gas (LPG), and infrared emitters [10]. This integration allows for process continuity during periods of low solar irradiance, and nighttime operation. Moreover, the coupling of auxiliary energy systems with control strategies enables improved regulation of drying conditions, contributing to more stable and efficient performance.

From a thermodynamic perspective, improving the performance of solar drying systems requires not only reducing energy consumption but also enhancing the portion of energy that can be effectively converted into work. In this regard, exergy analysis provides a rigorous framework for quantifying irreversibilities and identifying sources of thermodynamic inefficiency [11], thus contributing to mitigate entropy generation and environmental impacts.

Unlike conventional energy analysis, exergy-based approaches enable a more realistic assessment of system performance by accounting for the quality of energy flows. In addition, exergy analysis supports the development of sustainability indicators, such as the sustainability index (SI) and the exergy improvement factor (EIF), which offer further insight into the environmental and thermodynamic behavior of drying systems [12].

Notwithstanding its recognized potential, the application of exergy analysis to solar dryers is characterized by inconsistencies in the literature. Significant discrepancies exist in the formulation of exergy balances, the adopted assumptions, and the definition of performance indicators. These inconsistencies compromise the comparability of results and may lead to divergent interpretations of system performance.

A notable example concerns the evaluation of the exergy associated with the drying air stream. While some studies consider the drying agent as dry air [13–15], others treat it as a humid air mixture composed of dry air and water vapor [16–18]. Such differences in thermodynamic modeling directly affect the calculation of exergy flows and, consequently, the derived performance indicators. The lack of a standardized framework thus represents a critical gap in the literature.

In light of these challenges, this study presents a comprehensive and critical review of exergy-based performance evaluation in solar drying systems. The formulations employed in exergy balance equations are systematically examined, with emphasis on the definition of performance metrics and the assumptions underlying the estimation of useful exergy. The implications of alternative approaches are analyzed to establish a more consistent and reliable basis for the thermodynamic assessment and comparison of solar dryers.

2. Hybrid, Active and Indirect Solar Dryers

Active and indirect solar dryers typically consist of three main components: a solar collector for heating the air, a fan to provide forced airflow, and a drying chamber where the material is processed. The solar collector is installed at a specific tilt angle to maximize solar radiation absorption throughout the year, considering the geographical latitude of the installation site [19]. A schematic representation of an indirect solar dryer, based on the system investigated by Andrade [20], is shown in **Figure 1**.

In this configuration, solar radiation (1) passes through the transparent glass cover (2) and reaches the absorber plate (4), which may be flat, corrugated, or equipped with baffles. Corrugated surfaces or the inclusion of baffles increase the effective heat transfer area and promote airflow turbulence, thereby enhancing convective heat transfer to the working fluid [21–23].

The absorber plate is commonly made of aluminum or other material with high absorptivity and emissivity, it is typically coated with black paint to maximize solar energy absorption. Depending on the design, the plate may be located at the base of the collector, where airflow occurs over its surface, or centrally positioned within the collector enclosure, allowing air to be heated on both sides. The heated air is subsequently directed into the drying chamber, where it transfers heat and removes moisture from the product (11) by convection [24].

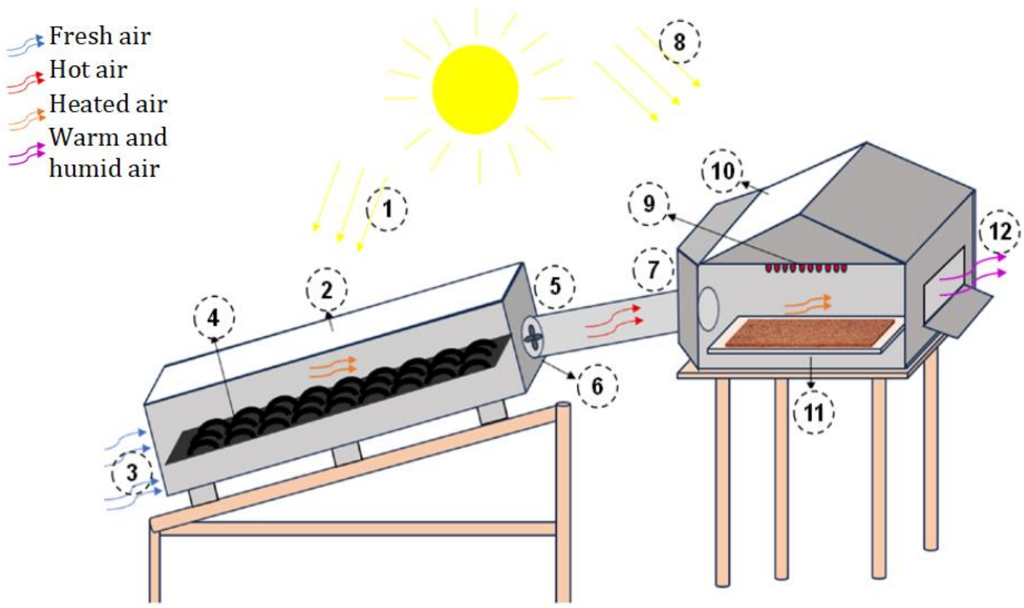

Figure 1. Schematic view of hybrid solar dryer. ① Solar radiation incident on the collector, ② Transparent glass cover, ③ Fresh air inlet, ④ Absorber plate, ⑤ Hot air outlet from collector, ⑥ Fan, ⑦ Hot air inlet in chamber, ⑧ Solar radiation incident on the chamber, ⑨ Infrared lamp, ⑩ Transparent glass cover of chamber, ⑪ Biomass tray, ⑫ Warm and humid air exhaust.

In forced convection systems, air circulation is typically achieved using a fan (6) or a blower. Lower airflow rates generally lead to higher air temperatures in the collector, while also enabling more compact system designs and reduced costs [25].

Depending on the design, a supplementary heating system may also be included, such as ohmic resistances or an infrared radiation source (9), among others. This results in what are referred to as hybrid dryers.

Depending on the system configuration, supplementary heating sources may be incorporated, such as electrical resistances or infrared radiation emitters (9), resulting in hybrid dryer configurations. These systems are designed to enhance drying rates and ensure continuous operation during periods of low solar radiation [26].

In addition, mixed-mode drying systems can be employed, in which the biomass (11) is heated both by convection from the drying air and by direct solar radiation (8) transmitted through a transparent cover (10).

3. Solar Dryer Performance Based on Exergy Analysis

The performance of solar dryers can be more comprehensively assessed by considering exergy, a thermodynamic property that accounts for both the quantity and quality of energy. In many studies, performance evaluation is restricted to conventional energy analysis, which neglects the degradation of energy during the process. Exergy analysis overcomes this limitation by explicitly quantifying irreversibilities and the useful work potential of the system.

The total exergy (E_X) of a system can be expressed as the sum of several contributions, including internal energy, entropy, work interactions, kinetic and potential energies, and chemical energy [19,27,28]:

$$E_X = (U - U_0) - T_0\,(S - S_0) + P_0\,(V - V_0) + V\,(P - P_0) + m\frac{v^2}{2} + mg\,(z - z_0) + \sum \left(\mu_i - \mu_{i,0}\right) n_i + \ldots \quad (1)$$

where U is the internal energy (J), S is the entropy (J·K^{-1}), T_0 is the ambient (reference) temperature (K), P is the system pressure (Pa), V is the total volume (m^3), m is the mass (kg), v is the velocity (m·s^{-1}), g is the gravitational acceleration (m·s^{-2}), and z is the elevation (m). The terms μ_i and n_i represent the chemical potential (J·mol^{-1}) and the number of moles (mol) of species i, respectively. Subscript "0" denotes properties evaluated at the reference (dead) state.

For a given system, the contribution of each term must be evaluated according to the level of detail required. In practical applications, certain terms—such as kinetic and potential exergy—are often negligible and can be omitted without significant loss of accuracy [29]. Furthermore, the internal energy and flow work terms are frequently combined into the enthalpy (H) term for convenience [19].

Exergy establishes a relationship between the amount of useful energy (or work) extracted and the total useful energy supplied by a given source. The portion of energy that is not converted into useful work within a system is associated with process irreversibilities and is defined as exergy destruction. The evaluation of these quantities is based on the exergy balance applied to a control volume, which can be written in rate form as [30]:

$$\dot{E}_{X,in} - \dot{E}_{X,out} - \dot{E}_{X,destr} = \mathrm{d}E_X/\mathrm{d}t \tag{2}$$

where the inlet ($\dot{E}_{X,in}$)and outlet ($\dot{E}_{X,out}$) rates account for exergy transfer by heat, mass flow, and work interactions. $\dot{E}_{X,destr}$ is the rate of destroyed exergy, and $\mathrm{d}E_X/\mathrm{d}t$ represents the rate of exergy accumulation.

In solar drying systems, exergy transfer is primarily associated with heat and mass interactions. The following section focuses on these mechanisms, with emphasis on their role in the thermodynamic evaluation of drying performance.

3.1. Exergy Transfer by Heat

In solar drying systems, exergy transfer by heat occurs primarily in the solar collector due to direct exposure to solar radiation. It may also occur in the drying chamber, through direct solar absorption (e.g., in mixed-mode or greenhouse dryers) or auxiliary heating sources such as infrared (IR) emitters.

The exergy transfer associated with heat interactions ($\dot{E}_{X,heat}$) is commonly evaluated using:

$$\dot{E}_{X,heat} = \left[1 - \frac{T_0}{T_s}\right] q \tag{3}$$

where q is the heat transfer rate, T_0 is the reference temperature, and T_S is the source temperature. This formulation is widely applied to conduction and convection processes [31] and is frequently used to estimate the exergy associated with moisture evaporation from the product ($\dot{E}_{X,ev}$) [16,32,33]. In such cases, it is expressed as:

$$\dot{E}_{X,ev} = \left[1 - \frac{T_0}{T_p}\right] e_{ev} \tag{4}$$

where T_p is the product temperature and e_{ev} denotes the rate of energy required for moisture evaporation, typically calculated from the latent heat of vaporization and the rate of water removal.

This same formulation has also been extended to quantify exergy transfer due to incident solar radiation ($\dot{E}_{X,solar}$):

$$\dot{E}_{X,solar} = \left[1 - \frac{T_0}{T_s}\right] q_{solar} \tag{5}$$

However, its application in this context raises important conceptual and methodological issues.

First, the solar temperature (T_s) is often inconsistently defined or not reported. Reported values range from 4,350 K to 6,000 K [16,33–37], introducing significant variability and limiting the comparability of exergy-based performance indicators.

Second, different formulations are used to estimate the incident solar energy rate (q_{solar}). The simplest approach assumes [38–40]:

$$q_{solar} = A_c I \tag{6}$$

where I is the solar irradiance and A_c is the collector area. A more physically representative expression incorporates optical properties [18,33,35]:

$$q_{solar} = \tau \alpha A_c I \tag{7}$$

where τ and α are the transmittance and absorptance, respectively. Neglecting these parameters leads to an overestimation of the effective energy input and, consequently, of exergy efficiency.

More fundamentally, the use of the previous heat-based formulation for solar radiation is theoretically inconsistent. The term $(1 - T_0/T_s)$, originally proposed by Jeter [41], is analogous to a Carnot efficiency factor and assumes heat transfer between two reservoirs in direct thermal contact [31]. This assumption is not valid for radiative transfer from the sun, where energy is transmitted through electromagnetic radiation rather than through a classical thermal interaction. As a result, the application of this expression to solar radiation may lead to significant deviations from the actual exergy content.

To address this limitation, several studies [40, 42] adopt an alternative formulation derived from radiation theory (Petela model) [43]:

$$\dot{E}_{X,solar} = \left[1 - \frac{4}{3}\left(\frac{T_0}{T_s}\right) + \frac{1}{3}\left(\frac{T_0}{T_s}\right)^4\right] q_{solar} \quad (8)$$

This expression more accurately represents the exergy of thermal radiation and is therefore more appropriate for solar-driven processes. Nevertheless, similar inconsistencies persist regarding the choice and reporting of T_s, which remains a critical source of uncertainty.

In hybrid solar dryers, analogous formulations are also applied to artificial infrared radiation sources. In this case, the exergy of absorbed radiation ($\dot{E}_{X,IR,abs}$) is commonly expressed using a quality factor [44]:

$$\dot{E}_{X,IR,abs} = \beta \cdot q_{IR,abs} \quad (9)$$

where the quality factor β accounts for the thermodynamic quality of radiation:

$$\beta = \left[1 - \frac{4}{3}\varepsilon_{IR}^{-0.25}\left(\frac{T_0}{T_{IR}}\right) + \frac{1}{3}\varepsilon_{IR}^{-1}\left(\frac{T_0}{T_{IR}}\right)^4\right] \quad (10)$$

The absorbed radiation $q_{IR,abs}$ is obtained from an energy balance within the drying chamber, accounting for incident, reflected, emitted, and transmitted components:

$$q_{IR,abs} = q_{IR,rad} - q_{IR,ref} - q_{IR,emit} - q_{IR,trans} \quad (11)$$

Its estimation can be further refined using radiation network analysis, which considers the geometric and radiative interactions between the infrared source, chamber walls, and product surface [31,44,45]:

$$q_{IR,abs} = \frac{\sigma\left(T_{IR}^4 - T_p^4\right)}{\frac{1-\varepsilon_{IR}}{A_{IR}\varepsilon_{IR}} + \frac{1}{\left(\frac{1}{A_{IR}F_{IR-p}}\right) + \left(\frac{1}{A_{IR}F_{IR-DC}}\right) + (1/A_pF_{p-DC})} + \frac{1-\varepsilon_p}{A_p\varepsilon_p}} \quad (12)$$

Each of the radiation components is illustrated in **Figure 2**.

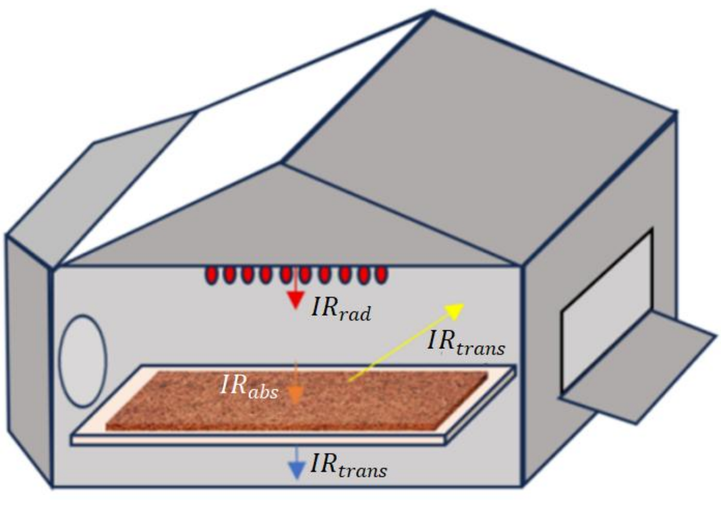

Figure 2. Artificial infrared radiation components in the drying chamber.

Tables 1 and **2** summarize studies that have applied Equations (5) and (8), respectively, to evaluate exergy transfer due to solar radiation.

Table 1. Studies employing Equation (5) for calculating exergy transfer due to solar radiation exposure.

Authors	Sun Temperature	Expression of q_{solar} in Equation (5)	Dryer Type
Hatami et al. [35]	4,350 K	Equation (7)	Indirect
Ndukwu et al. [37]	4,350 K	Equation (7)	Hybrid with auxiliary biomass furnace
Suherman et al. [40]	Not informed	Equation (6)	Hybrid with auxiliary biomass furnace
Bhardwaj et al. [46]	4,500 K	Equation (7)	Hybrid with auxiliary source: Phase Change Material (PCM)
Mugi and Chandramohan [36]	6,000 K	Equation (7)	Indirect
Arslan [27]	5,777 K	Equation (6)	Hybrid with auxiliary artificial infrared (IR) heating
Gilago et al. [14]	Not informed	Equation (7)	Indirect
Aghdam et al. [47]	6,000 K	Equation (6)	Indirect
Anuma et al. [48]	Not informed	Equation (7)	Direct (Greenhouse dryer)
Aqib et al. [39]	Not informed	Equation (6)	Hybrid with auxiliary sensible heat storage
Brahma et al. [49]	6,000 K	Equation (7)	Hybrid with auxiliary source: Phase Change Material (PCM)
Dutta et al. [13]	6,000 K	Equation (7)	Indirect
Ekka and Muthukumar [33]	4,500 K	Equation (7)	Mixed
Yazici and Kose [50]	Not informed	Equation (7)	Hybrid with auxiliary geothermal energy
Daliran et al. [51]	Not informed	Equation (7)	Direct (Greenhouse dryer)
Das et al. [52]	5,777 K	Equation (6)	Mixed
Deepak and Behura [53]	6,000 K	Equation (7)	Mixed
Barpatra Gohain et al. [16]	Not informed	Equation (7)	Hybrid with auxiliary biomass furnace

Table 2. Studies employing Equation (8) for calculating exergy transfer due to solar radiation exposure.

Authors	Sun Temperature	Expression of q_{solar} in Equation (8)	Dryer Type
Kiburi et al. [54]	Not informed	-	Hybrid with auxiliary source: biomass furnace
Hadibi et al. [15]	5,600 K	Equation (6)	Indirect with external PV panel
Heydari [55]	6,000 K	Equation (6)	Hybrid with auxiliary heating system
Abdelkader et al. [56]	5,600 K	Equation (6)	Hybrid with auxiliary source: Phase Change Material (PCM)
Malik and Kumar [42]	Not informed	Equation (6)	Mixed
Alktranee et al. [38]	Not informed	Equation (6)	Hybrid with auxiliary source: Phase Change Material (PCM)
*Flores-Prieto et al. [34]	5,600 K	Equation (7)	Hybrid with auxiliary source: water solar collector and electrical heater

Note: *This author employs a variation of Equation (1) in which a geometric factor is included.

3.2. Exergy Transfer by Mass Flow

Among the terms in the general exergy definition, Equation (1), the thermomechanical contribution is typically approximated by considering internal energy, flow work, and entropy [28]:

$$E_X = (U + PV) - (U_0 + P_0V_0) - T_0\,(S - S_0) \tag{13}$$

By replacing the first two components with the corresponding enthalpies, H and H_0, the equation is reduced to:

$$E_X = H - H_0 - T_0\,(S - S_0) \tag{14}$$

Assuming ideal-gas behavior for the drying air and expressing enthalpy as a function of temperature, the specific exergy ($e_{x,f}$) can be written as [30]:

$$e_{x,f} = c_{p,a}\,(T - T_0) - T_0\left[c_{p,a}ln\left(\frac{T}{T_0}\right) - R_a ln\left(\frac{P}{P_0}\right)\right] \tag{15}$$

Accordingly, the exergy rate associated with a mass flow stream ($\dot{E}_{X,f}$) is given by [34]:

$$\dot{E}_{X,f} = \dot{m}_a\left\{c_{p,a}\,(T - T_0) - T_0\left[c_{p,a}ln\left(\frac{T}{T_0}\right) - R_a ln\left(\frac{P}{P_0}\right)\right]\right\} \tag{16}$$

where $c_{p,a}$ is the specific heat of dry air at constant pressure, $\dot{m}_a$ is the airflow rate, and R_a is the specific gas constant for dry air.

In most solar drying applications, pressure variations relative to the reference state are negligible [49]. Under this assumption, the expression simplifies to:

$$\dot{E}_{X,f} = \dot{m}_a \left[c_{p,a}(T - T_0) - T_0 c_{p,a} ln\left(\frac{T}{T_0}\right)\right] \quad (17)$$

This simplified formulation is widely used to evaluate exergy transfer at the solar collector outlet and drying chamber boundaries. Among the 25 studies listed in **Tables 1** and **2**, 18 employed Equation (17). However, it relies on a key assumption: the drying agent is treated as dry air with negligible humidity [33]. While this approximation may be acceptable at the collector stage, it becomes increasingly inaccurate within the drying chamber, where the air is significantly enriched with water vapor.

To address this limitation, some studies [44,57] incorporate the effect of humidity by including water vapor properties:

$$\dot{E}_{X,f} = \dot{m}_a(c_{p,a} + Y \cdot c_{p,v})[(T - T_0) - T_o ln\left(\frac{T}{T_0}\right)] \quad (18)$$

where $c_{p,v}$ is the specific heat of water vapor at constant pressure, and Y is the absolute air humidity. Although this approach improves the thermodynamic representation of the drying air, it still neglects the contribution of chemical exergy contained in the flowing fluid [18,33,35]. This exergy is represented by the chemical potentials of the dry air (μ_a) and the water vapor (μ_v). Thus, for an ideal air–water vapor mixture, the specific molar exergy ($\overline{e}_x$) is given by [29]:

$$\overline{e}_x = x_a\left[\overline{h}_a - \overline{h}_{a,0} - T_0\left(\overline{s}_a - \overline{s}_{a,0}\right) + \mu_a - \mu_{a,0}\right] + x_v\left[\overline{h}_v - \overline{h}_{v,0} - T_0\left(\overline{s}_v - \overline{s}_{v,0}\right) + \mu_v - \mu_{v,0}\right] \quad (19)$$

where the enthalpy, entropy, and chemical potential terms for each component are determined as presented by Bejan [58]. The exergy of humid air per kg of dry air ($e_{x,f,ha}$) is then expressed as:

$$e_{x,f,ha} = \left(c_{p,a} + Y c_{p,v}\right)\left[(T - T_0) - T_0 ln\left(\frac{T}{T_0}\right)\right] + (1 + Y)R_a T_0 ln\left(\frac{P}{P_0}\right) + R_a T_0\left[ln\left(\frac{1+Y_0}{1+Y}\right) + Y ln\left(\frac{Y}{Y_0}\frac{1+Y_0}{1+Y}\right)\right] \quad (20)$$

This formulation accounts for both thermomechanical and chemical contributions, thus providing a more representative evaluation of exergy transfer in drying systems, particularly in the drying chamber, where mass and heat transfer processes are strongly coupled. By explicitly accounting for humidity effects and chemical potential, it reduces the inaccuracies associated with simplified models.

In addition to the exergy of the drying air, some studies [35,59] also evaluate the exergy associated with the moisture content of the product ($E_{X,w}$). Based on the general exergy expression, the specific exergy of water ($e_{x,w}$) can be written as:

$$e_{x,w} = h_w(T,P) - h_{w,0}(T_0, P_{w,0}) - T_0[s_w(T,P) - s_{w,0}(T_0, P_{w,0})] \quad (21)$$

where the reference partial pressure of water vapor ($P_{w,0}$) is defined as:

$$P_{w,0} = x_{v,0}P_0 = \left(\frac{Y_0}{1 + Y_0}\right)P_0 \quad (22)$$

Using approximations for the neighboring saturation state, as performed by Bejan [58], the exergy associated with the product moisture ($E_{X,w}$) can be expressed as [18]:

$$E_{X,w} = m_w\left\{\left[h_f(T) - h_g\,(T_0)\right] + v_f(T)\,[P - P_{sat}(T)] - T_0\left[s_f(T) + s_g\,(T_0)\right] + T_0 R_w ln\left[\frac{P_{sat}(T_0)}{x_{v,0}P_0}\right]\right\} \quad (23)$$

where m_w is the mass of evaporated water, $x_{v,0}$ is the molar fraction of water vapor at the reference state, and R_w is the specific gas constant for water vapor. Subscripts *"f"* and *"g"* refer to saturated liquid water and water vapor, respectively.

The inclusion of this exergy provides additional insight into the thermodynamic efficiency of the drying process, particularly in studies focusing on moisture removal mechanisms.

The widespread use of simplified formulations, particularly those neglecting humidity and chemical exergy, may lead to significant misinterpretation of system performance.

3.3. Exergy Efficiency

Although solar drying is inherently a transient process due to the continuous variation of solar radiation and ambient conditions, the adoption of steady-state assumptions remains a widely accepted approach in exergy analyses of both solar collector and drying chamber. This simplification allows the derivation of tractable formulations and facilitates the interpretation and comparison of performance indicators across different studies.

In practice, quasi-steady conditions can be assumed over short time intervals during which variations in operating parameters are relatively small. Under such conditions, instantaneous exergy rates can be evaluated as if the system were in steady state, providing meaningful insights into the thermodynamic behavior of the process.

Moreover, the steady-state framework enables the identification of dominant sources of irreversibility and supports the development of generalized performance criteria. Therefore, despite its inherent limitations, the steady-state assumption constitutes a reasonable and practical approximation for the exergy-based assessment of solar drying systems.

Under steady-state conditions, the exergy balance for a control volume reduces to:

$$\dot{E}_{X,in} - \dot{E}_{X,out} - \dot{E}_{X,destr} = 0 \tag{24}$$

Based on this relation, the exergy efficiency (η_{E_X}), is commonly defined as:

$$\eta_{E_X} = \frac{\dot{E}_{X,out}}{\dot{E}_{X,in}} = 1 - \frac{\dot{E}_{X,destr}}{\dot{E}_{X,in}} \tag{25}$$

In addition to exergy efficiency, several sustainability indicators [14] have been proposed to assess how the use of renewable energy in drying affects the environment [33]. Among these, the Sustainability Index (*SI*), Waste Energy Ratio (*WER*), Environmental Impact Factor (*EIF*), and Improvement Potential (*IP*) are widely used:

$$SI = \frac{1}{1 - \eta_{E_X}} \tag{26}$$

$$WER = \frac{\dot{E}_{X,destr}}{\dot{E}_{X,in}} \tag{27}$$

$$EIF = \frac{WER}{\eta_{E_X}} \tag{28}$$

$$IP = (1 - \eta_{E_x})\dot{E}_{X,destr} \tag{29}$$

These indicators provide complementary information on system performance, linking exergy destruction to environmental impact and improvement potential. For example, higher *SI* values are associated with systems exhibiting higher η_{E_X}, which results in lower entropy generation and, consequently, a reduced environmental impact. On the other hand, low values are desired for both *WER* and *EIF* indicators, since their formulations directly account for the exergy that is not utilized in the process and is therefore released into the environment [51,60].

The Improvement Potential (IP) assesses the extent to which the process can be improved by reducing destroyed exergy—and, consequently, irreversibilities [33]. Lower IP values indicate that the energy supplied to the process is being used more efficiently.

The following subsection presents formulations for the exergy efficiency of solar collectors and drying chambers commonly found in the literature.

3.3.1. Exergy Efficiency in Solar Collectors

In solar collectors, exergy efficiency ($\eta_{E_{X,c}}$) reflects the ability to convert incident solar radiation into useful exergy carried by the airflow. Thus, the higher the $\eta_{E_{X,c}}$, the greater the amount of useful exergy effectively applied for heating the drying agent. Several studies [33,36,53] have adopted the same definition of exergy efficiency for the solar collector:

$$\eta_{E_{X,c}} = \frac{\dot{m}_a C_{p,a}\left[(T_{co} - T_{ci}) - T_0 ln\left(\frac{T_{co}}{T_{ci}}\right)\right]}{\left[1 - \frac{T_0}{T_s}\right] \cdot \tau\alpha I A_c} \tag{30}$$

In this formulation, the exergy transferred due to solar radiation is based on a Carnot-type factor and incorporates optical properties, while the air-stream exergy is evaluated using the thermomechanical contributions based on ideal gas assumptions.

Mugi and Chandramohan [36] investigated both passive and active drying of guava slices in an indirect solar dryer. A higher average exergy efficiency of the collector was reported under active mode (3.74%) compared to passive mode (2.39%).

Deepak and Behura [53] used a mixed-mode solar dryer operating with either natural (NC) or forced (FC) air convection for drying tomato slices, obtaining relatively similar exergy efficiency values of 12.28% (FC mode) and 12.55% (NC mode).

Ekka and Muthukumar [33] evaluated thin layer drying of fig under forced air convection in a mixed-mode solar dryer equipped with two double-pass solar collectors connected in series. Despite the increase in exergy efficiency with air mass flow rate, the overall performance remained low, with maximum average values of 4.7% and 3.7% for collectors 1 and 2, respectively.

Ideally, the exergy supplied by solar radiation should be entirely transferred to the working fluid. However, reported values are typically low (often below 15%), indicating significant irreversibilities associated with heat losses, optical inefficiencies, and thermal resistance effects. Based on this, aspects related to process variables, equipment design, and other factors may be reconsidered in order to achieve a higher level of exergy utilization.

3.3.2. Exergy Efficiency in Drying Chambers

Existing formulations of exergy efficiency for drying chambers ($\eta_{E_{X,d}}$) vary significantly. Most studies define efficiency based on inlet and outlet airflow exergy:

$$\eta_{E_{X,d}} = \frac{\dot{E}_{X,f,do}}{\dot{E}_{X,f,di}} \tag{31}$$

From this relation, Ekka and Muthukumar [33] and Deepak and Behura [53] employed the same formulation for evaluating the exergy performance of mixed-mode solar dryers:

$$\eta_{E_{X,d}} = \frac{\dot{m}_a C_{p,a}\left[(T_{do} - T_0) - T_0 ln\left(\frac{T_{do}}{T_0}\right)\right]}{\dot{m}_a C_{p,a}\left[(T_{di} - T_0) - T_0 ln\left(\frac{T_{di}}{T_0}\right)\right] + \left[1 - \frac{T_0}{T_s}\right] \cdot \tau I A_d} \tag{32}$$

where the inlet term includes the exergy rate carried by the air heated in the collector as well as the exergy transfer associated with solar radiation incident on the drying chamber. The outlet term corresponds to the thermomechanical exergy of the air leaving the chamber.

A similar approach was adopted by Mugi and Chandramohan [36] in the evaluation of an indirect solar dryer. However, in their formulation, the exergy associated with the solar radiation incident on the chamber was not considered. A higher average exergy efficiency was observed in passive mode (57.03%) compared to active mode (50.92%). The corresponding improvement potential (IP) was lower in natural convection mode (4.22 W) than in forced convection mode (5.84 W), while the waste energy ratio (WER) values were 0.438 and 0.481, respectively. These results were attributed to the lower drying chamber temperatures observed at higher airflow rates under forced convection, which reduced the effectiveness of energy utilization during the drying process.

Deepak and Behura [53] reported average exergy efficiencies of 34.3% and 11.71% under forced and natural convection, respectively. The higher exergy destruction observed under natural convection resulted in a greater improvement potential (IP), with average values of 66.76 W compared to 50.36 W under forced convection.

Ekka and Muthukumar [33] observed that the exergy efficiency of the drying chamber increased with higher air mass flow rates, ranging from 18.8% to 41.4%.

Such results highlight the sensitivity of exergy-based performance indicators to airflow conditions and heat transfer characteristics within the drying chamber.

Şevik et al. [44] employed a hybrid solar dryer equipped with a double-pass solar collector for drying apple and mint slices. The supplementary energy was provided by infrared (IR) lamps. In their exergy analysis, the formulation accounted for both the presence of water vapor in the airflow and the exergy associated with IR heating within the drying chamber:

$$\eta_{E_{X,d}} = \frac{\dot{m}_a(C_{p,a} + Y_{do}C_{p,v})\left[(T_{do} - T_0) - T_0 ln\left(\frac{T_{do}}{T_0}\right)\right]}{\dot{m}_a(C_{p,a} + Y_{di}C_{p,v})\left[(T_{di} - T_0) - T_0 ln\left(\frac{T_{di}}{T_0}\right)\right] + \dot{E}_{X,IR,abs}} \quad (33)$$

where,

$$\dot{E}_{X,IR,abs} = \frac{\left[1 - \frac{4}{3}\varepsilon_{IR}^{-0.25}\left(\frac{T_0}{T_{IR}}\right) + \frac{1}{3}\varepsilon_{IR}^{-1}\left(\frac{T_0}{T_{IR}}\right)^4\right]\sigma\left(T_{IR}^4 - T_p^4\right)}{\frac{1-\varepsilon_{IR}}{A_{IR}\varepsilon_{IR}} + \frac{1}{\left(\frac{1}{A_{IR}F_{IR-p}}\right)+\left(\frac{1}{A_{IR}F_{IR-DC}}\right)+(1/A_pF_{p-DC})} + \frac{1-\varepsilon_p}{A_p\varepsilon_p}} \quad (34)$$

The values of $\eta_{E_{X,d}}$ for apple and mint drying were 59.1% and 49.2%, respectively.

Rather than analyzing exergy efficiency results, a critical discussion of the approaches adopted in the cited studies is presented.

Conventional definitions based solely on air-stream exergy present a conceptual limitation. In drying processes, the objective is not to preserve exergy in the airflow, but rather to transfer it for moisture removal and product heating. Consequently, focusing exclusively on the air stream leads to an assessment of exergy conservation rather than exergy utilization.

This approach effectively quantifies the fraction of exergy remaining in the air after the drying process, rather than the fraction that has been usefully employed.

A more physically consistent evaluation can be obtained by defining the useful exergy as the portion effectively utilized in the drying process. Thus, the drying exergy efficiency can be expressed as:

$$\eta_{E_{X,d}} = \frac{\dot{E}_{X,in} - \dot{E}_{X,out}}{\dot{E}_{X,in}} \quad (35)$$

This formulation represents the fraction of supplied exergy that is effectively consumed within the drying process. However, it should be noted that this term includes both useful exergy and irreversibilities. Therefore, a more rigorous definition should explicitly account for the exergy associated with drying.

Malik and Kumar [42] defined the exergy associated with moisture evaporation as the useful exergy, while the exergy associated with solar radiation was taken as the input exergy:

$$\eta_{E_{X,d}} = \frac{\frac{m_w}{3600}\left[\Delta H\left(1 - \frac{T_0}{T_p}\right)\right]}{IA_d\left[1 - \frac{4}{3}\left(\frac{T_0}{T_s}\right) + \frac{1}{3}\left(\frac{T_0}{T_s}\right)^4\right]} \quad (36)$$

The authors evaluated the performance of a vertical mixed-mode solar dryer equipped with a circular solar collector for drying turmeric under both natural and forced airflow conditions. The exergy efficiency under forced convection was 2.01%, representing an increase of 1.99% compared to natural convection. Moreover, no significant differences were observed in the waste energy ratio (WER) and sustainability index (SI), with values of 0.980 and 1.020, respectively.

Formulations that incorporate the exergy associated with latent heat of vaporization of free water (ΔH) improve the representation of the useful exergy involved in drying. Nevertheless, the exergy requirement for drying is not limited to free water evaporation, since most porous solids dry predominantly during the falling-rate period. Consequently, additional exergy is required to remove bound water.

Therefore, it is recommended to use the heat of desorption (ΔH_{des}) instead of the latent heat of vaporization of free water, in order to avoid that part of useful exergy is considered as irreversibility.

Another approach, adopted by Hatami et al. [35], defines the exergy efficiency of the drying process as the ratio of the changes in the moisture exergy of the product to its initial moisture exergy:

$$\eta_{E_{X,d}} = \frac{E_{X_{w,1}} - E_{X_{w,2}}}{E_{X_{w,1}}} \tag{37}$$

where $E_{X_{w,1}}$ and $E_{X_{w,2}}$ are evaluated from Equation (23).

Hatami et al. [35] evaluated the exergy performance of drying in an indirect solar dryer as a function of time and moisture content. The analysis accounted for incident solar radiation, temperature variation along the collector, and changes in both solid temperature and moisture content. The drying exergy efficiency was found to decrease with increasing air mass flow rate. This behavior was attributed to the reduction in drying chamber and product temperatures, which limited the evaporation capacity of the material. Moreover, the highest efficiency values at all flow rates were observed near the critical moisture content.

The study also showed that the exergy efficiency was not affected by the amount of drying material, which represents an advantage over formulations based on variations in air-stream exergy. Therefore, moisture-based exergy formulations can contribute to a more intrinsic understanding of drying system performance, as they are independent of the processed material mass.

The formulation given by the Equation (36) incorporates the exergy associated with latent heat of vaporization of free water, thereby providing a closer representation of the useful energy involved in moisture removal. Similarly, the approach adopted in Equation (37), based on the exergy of the product moisture content, offers a more direct assessment of drying performance, as it focuses on the thermodynamic state of the material itself.

However, none of these formulations simultaneously accounts for both desorption and sensible heat contributions in a unified framework. To address this limitation, a process-based exergy efficiency is proposed, in which the useful exergy is defined as the fraction effectively employed in the drying:

$$\eta_{E_{X,d}} = \frac{E_{X,useful}}{E_{X,in}} \tag{38}$$

where the useful exergy ($E_{X,useful}$) is given by the sum of the exergy associated with moisture desorption and product heating:

$$E_{X,useful} = E_{X,des} + E_{X,sens} \tag{39}$$

The exergy associated with moisture desorption ($E_{X,des}$) is defined as:

$$E_{X,des} = m_w \left(1 - \frac{T_0}{T_p}\right) \Delta H_{des} \tag{40}$$

while the exergy associated with product heating ($E_{X,sens}$) is expressed as:

$$E_{X,sens} = m_p c_{p,p} \left[(T_p - T_0) - T_0 \ln\left(\frac{T_p}{T_0}\right)\right] \tag{41}$$

When combined with sustainability indicators, the exergy efficiency derived from this approach enables the quantification of both the useful exergy harnessed and the exergy released to the environment. This, in turn, allows for the evaluation of whether the selected process parameters and system design effectively maximize the utilization of useful exergy during drying.

The proposed formulation extends previous approaches by explicitly incorporating the main mechanisms responsible for exergy consumption during drying. As a result, it enables a more comprehensive and physically consistent evaluation of system performance, while improving the comparability of results across different studies.

Overall, the analysis indicates that the definition of exergy efficiency is not merely a mathematical choice, but a fundamental aspect that determines how system performance is interpreted.

3.3.3. Role of Monitoring and Control

Rasheed et al. [61] automated a hybrid solar dryer by controlling the temperature through manipulation of the drying-air flow rate. The results showed increases of 31% and 15% in the average collector and drying efficiencies, respectively.

Hidra et al. [62] developed a monitoring and control framework for a hybrid solar dryer to enhance the drying of agricultural products. A Proportional–Integral–Derivative (PID) controller was applied to regulate the temperature by actuating the heating elements. The peak drying efficiency was of 89%.

These recent studies highlight the importance of real-time monitoring and control strategies for improving drying efficiency. The use of sensors associated with a data acquisition and processing system enables continuous monitoring of process variables as well as of performance parameters. Furthermore, integration of sensors and control systems enables continuous adjustment of operating conditions, reducing irreversibilities and enhancing system performance.

4. Conclusions

This study presented a critical assessment of exergy-based performance evaluation in solar drying systems, with particular emphasis on the definitions, assumptions, and formulations employed in the literature. The analysis revealed a lack of standardization in the evaluation of exergy efficiency, especially regarding the definition of useful exergy. Most existing approaches rely on air-stream exergy at the dryer outlet, which, although mathematically consistent, does not adequately represent the fundamental objective of the drying process—namely, the effective utilization of energy for moisture removal.

Significant discrepancies were also identified in the calculation of exergy transfer by heat and mass flow, including the selection of solar temperature, the formulation of incident radiation terms, and the treatment of the drying agent as either dry air or an air–vapor mixture. These variations hinder the comparability of results across studies and may lead to inconsistent interpretations of system performance.

To address these limitations, a process-based exergy efficiency was proposed, in which the useful exergy is defined as the sum of the contributions associated with moisture desorption and product heating. This formulation provides a more physically meaningful representation of the drying process, as it directly quantifies the exergy effectively utilized rather than the exergy remaining in the working fluid. By explicitly linking exergy consumption to the underlying drying mechanisms, the proposed approach enables a more accurate assessment of system performance and supports more reliable comparisons between different dryer configurations and operating conditions.

In addition, the integration of sustainability indicators such as the sustainability index, waste energy ratio, environmental impact factor, and improvement potential was shown to provide complementary insights into the thermodynamic and environmental performance of solar dryers. These parameters, when used alongside a consistent definition of exergy efficiency, can support the identification of inefficiencies and guide system optimization.

From a practical perspective, the findings highlight the importance of adopting more rigorous methodologies in exergy analysis, including the continuous monitoring of product temperature and moisture content, as well as the evaluation of the drying agent as a humid air mixture. Furthermore, the implementation of monitoring and control strategies was identified as a promising pathway for reducing irreversibilities and enhancing system performance.

Overall, this work contributes to advancing the thermodynamic assessment of solar drying systems by providing a critical synthesis of existing approaches and proposing a more consistent framework for exergy-based performance evaluation. The adoption of the proposed formulation may support the development of more efficient, sustainable, and comparable solar drying technologies in future research.

Author Contributions

Conceptualization, M.M.d.P. and K.S.A.; methodology, K.S.A. and G.A.C.; validation, K.S.A. and G.A.C.; formal analysis, M.M.d.P.; investigation, K.S.A. and G.A.C.; resources, G.A.C. and M.F.F.S.; data curation, K.S.A. and G.A.C.; writing—original draft preparation, K.S.A. and G.A.C.; writing—review and editing, M.M.d.P. and M.F.F.S.; supervision, M.M.d.P. All authors have read and agreed to the published version of the manuscript.

Funding

This work was funded by the National Council for Scientific and Technological Development (CNPq) and Coordination for the Improvement of Higher Education Personnel (CAPES).

Institutional Review Board Statement

Not applicable.

Informed Consent Statement

Not applicable.

Data Availability Statement

No new data were created in this work.

Acknowledgments

The authors would like to express their gratitude to CNPq and CAPES for the financial support.

Conflicts of Interest

The authors declare no conflict of interest.

AI Use Statement

During the preparation of this work the authors used ChatGPT, an AI-based translation tool, in order to improve the translation of the text into English. No AI tools were used for data analysis, interpretation, or generation of scientific content. After using this tool/service, the authors reviewed and edited the content as needed and take full responsibility for the content of the published article.

Abbreviations

Abbreviation	**Full Name**
A_c	Collector surface area (m^2)
A_d	Drying chamber area (m^2)
A_{IR}	Infrared source area (m^2)
A_p	Product area (m^2)
$c_{p,a}$	Specific heat capacity of dry air at constant pressure ($J/kg\ K$)
$c_{p,p}$	Specific heat capacity of product at constant pressure ($J/kg\ K$)
$c_{p,v}$	Specific heat capacity of water vapor at constant pressure ($J/kg\ K$)
e_{ev}	Rate of energy used for water evaporation (W)
$\overline{e_x}$	Specific molar exergy (J/mol)
E_X	Exergy (J)
$E_{X,des}$	Moisture desorption-based exergy (J)
$\dot{E}_{X,destr}$	Rate of exergy destroyed (W)
$\dot{E}_{X,ev}$	Exergy transfer rate by evaporation (W)
$e_{x,f}$	Specific flow exergy (J/kg)
$e_{x,f,ha}$	Specific flow exergy of humid air (J/kg)
$\dot{E}_{X,f}$	Exergy transfer rate by flow (W)
$\dot{E}_{X,f,di}$	Exergy rate due flow entering cabin (W)
$\dot{E}_{X,f,do}$	Exergy rate due flow leaving cabin (W)
$\dot{E}_{X,heat}$	Exergy transfer rate by heat (W)
$\dot{E}_{X,in}$	Exergy rate entering the system (W)
$\dot{E}_{X,IR,abs}$	Rate of absorbed infrared exergy (J)
$\dot{E}_{X,out}$	Exergy rate leaving the system (W)
$\dot{E}_{X,solar}$	Exergy rate by solar radiation (W)
$E_{X,sens}$	Exergy associated with product heating (J)
$E_{X,useful}$	Useful exergy (J)
$e_{x,w}$	Specific exergy from solid moisture (J/kg)

$E_{X,w}$	Exergy from product moisture (J)
EIF	Environmental Impact Factor (-)
FC	Forced convection
$F_{IR\text{-}DC}$	Shape factor IR source–drying chamber (-)
$F_{IR\text{-}p}$	Shape factor IR source–product (-)
$F_{p\text{-}DC}$	Shape factor product–drying chamber
g	Gravity acceleration (m/s^2)
H	Enthalpy (J)
H_0	Enthalpy at reference state (J)
$\overline{h}_a$	Molar enthalpy of dry air (J/mol)
$\overline{h}_{a,0}$	Molar enthalpy of dry air at reference state (J/mol)
h_f	Specific enthalpy of saturated liquid water (J/kg)
h_g	Specific enthalpy of saturated water vapor (J/kg)
$\overline{h}_v$	Molar enthalpy of water vapor (J/mol)
$\overline{h}_{v,0}$	Molar enthalpy of water vapor at reference state (J/mol)
h_w	specific enthalpy of water (J/kg)
$h_{w,0}$	specific enthalpy of water at reference state (J/kg)
I	Instantaneous solar radiation (W/m^2)
IP	Improvement Potential (W)
IR	Infrared
m	Mass (kg)
$\dot{m}_a$	Air mass flow rate (kg/s)
m_w	Quantity of evaporated water (kg)
n_i	number of moles of component i(mol)
NC	Natural Convection
P	Pressure (Pa)
P_0	Reference pressure (Pa)
P_{sat}	Saturation pressure of water (Pa)
$P_{w,0}$	Partial pressure of water in the ambient air (Pa)
q	Heat transfer heat (W)
q_{IR}	Rate of IR radiation (W)
$q_{IR,abs}$	Rate of IR radiation absorbed (W)
$q_{IR,emit}$	Rate of IR radiation emitted by solid (W)
$q_{IR,rad}$	Total rate of IR radiation emitted by source (W)
$q_{IR,ref}$	Rate of IR heat reflected by material (W)
$q_{IR,trans}$	Rate of IR radiation transmitted (W)
q_{solar}	Rate of incident solar radiation (W)
R_a	Specific gas constant of dry air ($J/kg{\cdot}K$)
R_w	Specific gas constant of water vapor ($J/kg{\cdot}K$)
S	Entropy (J/K)
S_0	Entropy at reference state ($J/kg\ K$)
$\overline{s}_a$	Molar entropy of dry air ($J/mol{\cdot}K$)
$\overline{s}_{a,0}$	Molar entropy of dry air at reference state ($J/mol{\cdot}K$)
s_f	Specific entropy of saturated liquid water ($J/kg\ K$)
s_g	Specific entropy of saturated water vapor ($J/kg\ K$)
$\overline{s}_v$	Molar entropy of water vapor ($J/mol{\cdot}K$)
$\overline{s}_{v,0}$	Molar entropy of water vapor at reference state (J/mol K)
s_w	Specific entropy of water ($J/kg\ K$)
$s_{w,0}$	Specific entropy of water at reference state ($J/kg\ K$)
SI	Sustainability Index (-)
t	Time (s)

T	Temperature (K)
T_0	Reference temperature (K)
T_{ci}	Air temperature at the collector inlet (K)
T_{co}	Air temperature at the collector outlet (K)
T_{di}	Air temperature at the chamber inlet (K)
T_{do}	Air temperature at the chamber outlet (K)
T_{IR}	Infrared radiation source temperature (K)
T_p	Product temperature (K)
T_S	Source temperature (or sun) (K)
U	Internal energy (J)
U_0	Internal energy at reference state (J)
v	Velocity (m/s)
v_f	specific volume of saturated liquid water (m^3/kg)
V	Volume (m^3)
V_0	Reference volume (m^3)
WER	Waste energy ratio (-)
x_a	Molar fraction of dry air (-)
x_v	Molar fraction of water vapor (-)
$x_{v,0}$	mole fraction of water vapor in the reference environment (–)
Y	Absolute air humidity ($kg_{water}/kg_{dry\ air}$)
Y_0	Absolute air humidity at reference state ($kg_{water}/kg_{dry\ air}$)
Y_{di}	Absolute air humidity at the chamber drying inlet ($kg_{water}/kg_{dry\ air}$)
Y_{do}	Absolute air humidity at the drying chamber outlet ($kg_{water}/kg_{dry\ air}$)
z	Elevation (m)
z_0	Reference elevation (m)
α	Absorptance (-)
β	Quality factor
ΔH	Latent heat of vaporization of free water (J/kg)
ΔH_{des}	Heat of desorption of moisture (J/kg)
ε_{IR}	Infrared source emissivity (-)
ε_p	Product emissivity (-)
η_{E_X}	Exergy efficiency (-)
$\eta_{E_{X,c}}$	Solar collector exergy efficiency (-)
$\eta_{E_{X,d}}$	Drying chamber exergy efficiency (-)
μ_a	Chemical potential of dry air in the mixture (J/mol)
$\mu_{a,0}$	Chemical potential of dry air at the thermodynamics dead state (J/mol)
μ_i	Chemical potential of component *i* in the mixture (J/mol)
$\mu_{i,0}$	Chemical potential of component *i* at the thermodynamics dead state (J/mol)
μ_v	Chemical potential of water vapor in the mixture (J/mol)
$\mu_{v,0}$	chemical potential of water vapor at the thermodynamics dead state (J/mol)
σ	Stephan–Boltzmann constant (W/m^2K^4)
τ	Transmittance (-)

References

1. Chojnacka, K.; Mikula, K.; Izydorczyk, G.; et al. Improvements in Drying Technologies—Efficient Solutions for Cleaner Production with Higher Energy Efficiency and Reduced Emission. *J. Clean. Prod.* **2021**, *320*, 128706. [CrossRef]
2. Faria, D.J.; Carvalho, A.P.A.d.; Conte-Junior, C.A. Fermentation of Biomass and Residues from Brazilian Agriculture for 2G Bioethanol Production. *ACS Omega* **2024**, *9*, 40298–40314. [CrossRef]
3. Gunasekaran, D.L.; Duraisamy, S. Experimental Investigation and 4E+Q (Energy, Exergy, Economic, Environmental, and Quality) Analysis of a Novel Solar Evacuated Tube Dryer. *Sol. Energy* **2026**, *303*, 114080. [CrossRef]

4. Nettari, C.; Benseddik, A.; Boubekri, A.; et al. Energy and Exergy Analysis and Drying Kinetics of Pumpkins in a Medium-Size Solar Cabinet Dryer Enhanced with Heat Recovery and Sensible Heat Storage. *J. Energy Storage* **2026**, *143*, 119749. [CrossRef]
5. Rajesh, S.; Madhankumar, S.; Arunkumar, P.M.; et al. Drying Kinetics, Energy, Exergy, and Economic Aspects of Indirect Solar Dryer with Phase Change Material. *Sol. Energy* **2026**, *305*, 114287. [CrossRef]
6. Alsakran, A.A.; Younis, O.S.; Székács, A.; et al. CFD, Energy, and Exergy Analysis and Sustainability Indicators of Tilapia Fish Strips Drying Using an Evacuated Tubes Indirect Solar Dryer. *Sci. Rep.* **2025**, *15*, 25893. [CrossRef]
7. Anyaoha, C.O.; Okoroigwe, F.C.; Okoroigwe, C.N.; et al. A Review of Optimization Strategies for Solar-Biomass Dryers. *Sustain. Energy Technol. Assess.* **2025**, *83*, 104672. [CrossRef]
8. Rashid, F.L.; Hammoodi, K.A.; Al Maimuri, N.M.L.; et al. Recent Advancements in Hybrid Solar Dryer: A Comprehensive Review of Integration Strategies, Performance Enhancements, and Applications. *Int. Commun. Heat Mass Transf.* **2026**, *171*, 110042. [CrossRef]
9. Salami, P.; Safvati, M.; Barghi Jahromi, M.S.; et al. Classification of Fruit Solar Dryers and the Role of Phase Change Materials in Enhancing Performance: A Review. *Sol. Energy* **2025**, *297*, 113570. [CrossRef]
10. Saha, C.K.; Roy, N.K.; Khatun, J.; et al. Solar Hybrid Dryers for Fruits, Vegetables, and Fish: A Comprehensive Review on Constructional Features and Techno-Economic-Environmental Analysis. *Sustain. Energy Technol. Assess.* **2024**, *68*, 103878. [CrossRef]
11. Prajapati, P.; Raja, B.D.; Savaliya, H.; et al. Thermodynamic Evaluation of Shell and Tube Heat Exchanger through Advanced Exergy Analysis. *Energy* **2024**, *292*, 130421. [CrossRef]
12. Qamar, Z.; Munir, A.; Amjad, W.; et al. Energy and Exergy Analyses of a Solar Assisted Milk Powder Spray Dryer. *Therm. Sci. Eng. Prog.* **2025**, *57*, 103131. [CrossRef]
13. Dutta, P.; Das, H.; Dutta, P.P.; et al. Evaluation of an Improved Indirect Solar Dryer for Curcuma Amada without and with Stone Chips as Thermal Energy Storage: An Investigation on Kinetics, Energy, Exergy, Quality and Economic Aspects. *J. Energy Storage* **2024**, *79*, 110199. [CrossRef]
14. Gilago, M.C.; Mugi, V.R.; Chandramohan, V.P. Evaluating the Environ-Economic and Exergy-Energy Impacts of Drying Carrots in Passive and Active Mode Solar Dryers. *Therm. Sci. Eng. Prog.* **2023**, *43*, 101956. [CrossRef]
15. Hadibi, T.; Mennouche, D.; Boubekri, A.; et al. Drying Characteristic, Sustainability, and 4E (Energy, Exergy, and Enviro-Economic) Analysis of Dried Date Fruits Using Indirect Solar-Electric Dryer: An Experimental Investigation. *Renew. Energy* **2023**, *218*, 119291. [CrossRef]
16. Barpatra Gohain, R.J.; Dutta, P.P.; Bora, N. Exergy, Economic and Environmental Impacts Analysis of a Solar-Biomass Powered Hybrid Dryer for Drying Eryngium Foetidum. *Therm. Sci. Eng. Prog.* **2025**, *59*, 103325. [CrossRef]
17. Ndukwu, M.C.; Augustine, E.B.; Ugwu, E.; et al. Drying Kinetics and Thermo-Economic Analysis of Drying Hot Water Blanched Ginger Rhizomes in a Hybrid Composite Solar Dryer with Heat Exchanger. *Heliyon* **2023**, *9*, e13606. [CrossRef]
18. Nwakuba, N.; Okafor, V.C.; Okorafor, O.O. Techno-Economic Analysis of a Hybrid Solar-Electric Dryer. *Energy Sources Part Recovery Util. Environ. Eff.* **2020**, *46*, 10289–10313. [CrossRef]
19. Lingayat, A.B.; Chandramohan, V.P.; Raju, V.R.K.; et al. A Review on Indirect Type Solar Dryers for Agricultural Crops—Dryer Setup, Its Performance, Energy Storage and Important Highlights. *Appl. Energy* **2020**, *258*, 114005. [CrossRef]
20. Andrade, K.S. Design, Construction and Performance Evaluation of a Hybrid Solar Dryer for Drying Cassava Peel. Master's Thesis, Universidade Federal de Sergipe, São Cristóvão, Brazil, 2024. (in Portuguese)
21. Nidhul, K.; Kumar, S.; Yadav, A.K.; et al. Computational and Experimental Studies on the Development of an Energy-Efficient Drier Using Ribbed Triangular Duct Solar Air Heater. *Sol. Energy* **2020**, *209*, 454–469. [CrossRef]
22. Nidhul, K.; Yadav, A.K.; Anish, S.; et al. Thermo-Hydraulic and Exergetic Performance of a Cost-Effective Solar Air Heater: CFD and Experimental Study. *Renew. Energy* **2022**, *184*, 627–641. [CrossRef]
23. Prajapati, S.; Naik, N.; Chandramohan, V.P. Numerical Solution of Solar Air Heater with Triangular Corrugations for Indirect Solar Dryer: Influence of Pitch and an Optimized Pitch of Corrugation for Enhanced Performance. *Sol. Energy* **2022**, *243*, 1–12. [CrossRef]
24. Mohana, Y.; Mohanapriya, R.; Anukiruthika, T.; et al. Solar Dryers for Food Applications: Concepts, Designs, and Recent Advances. *Sol. Energy* **2020**, *208*, 321–344. [CrossRef]
25. Duffie, J.A.; Beckman, W.A. *Solar Engineering of Thermal Processes*, 1st ed.; Wiley: Hoboken, NJ, USA, 2013.
26. Nnamchi, O.; Tom, C.; Akpan, G.; et al. Solar Dryers: A Review of Mechanism, Methods and Critical Analysis of Transport Models Applicable in Solar Drying of Product. *Green Energy Resour.* **2025**, *3*, 100118. [CrossRef]

27. Arslan, E. Experimental Performance Analysis of Infrared Assisted Solar Air Heater for Continuous Applications of Drying. *Energy Sources Part A Recover. Util. Environ. Eff.* **2023**, *45*, 1168–1185. [CrossRef]
28. César, L.-V.E.; Ana Lilia, C.-M.; Octavio, G.-V.; et al. Energy and Exergy Analyses of a Mixed-Mode Solar Dryer of Pear Slices (*Pyrus Communis* L). *Energy* **2021**, *220*, 119740. [CrossRef]
29. Niksiar, A.; Rahimi, A. Energy and Exergy Analysis for Cocurrent Gas Spray Cooling Systems Based on the Results of Mathematical Modeling and Simulation. *Energy* **2009**, *34*, 14–21. [CrossRef]
30. Çengel, Y.A.; Boles, M.A. *Thermodynamics*, 7th ed.; Amgh: Porto Alegre, Brazil, 2021. (in Portuguese)
31. Mohammed, H.N.; Mengüç, M.P. Exergy Efficiency for Radiation Heat Transfer. *IOP Conf. Ser. Mater. Sci. Eng*. **2020**, *671*, 012022. [CrossRef]
32. Aghbashlo, M. Exergetic Simulation of a Combined Infrared-Convective Drying Process. *Heat Mass Transf.* **2016**, *52*, 829–844. [CrossRef]
33. Ekka, J.P.; Muthukumar, P. Exergy Efficiency and Sustainability Indicators of Forced Convection Mixed Mode Solar Dryer System for Drying Process. *Renew. Energy* **2024**, *234*, 121256. [CrossRef]
34. Flores-Prieto, J.J.; Hernandez, J.A.; Huicochea, A. Energy and Exergy Analysis of a Hybrid Dryer with Air/Water Solar Collectors. *Energy* **2025**, *332*, 137076. [CrossRef]
35. Hatami, S.; Payganeh, G.; Mehrpanahi, A. Energy and Exergy Analysis of an Indirect Solar Dryer Based on a Dynamic Model. *J. Clean. Prod.* **2020**, *244*, 118809. [CrossRef]
36. Mugi, V.R.; Chandramohan, V.P. Energy, Exergy and Economic Analysis of an Indirect Type Solar Dryer Using Green Chilli: A Comparative Assessment of Forced and Natural Convection. *Therm. Sci. Eng. Prog.* **2021**, *24*, 100950. [CrossRef]
37. Ndukwu, M.C.; Simo-Tagne, M.; Abam, F.I.; et al. Exergetic Sustainability and Economic Analysis of Hybrid Solar-Biomass Dryer Integrated with Copper Tubing as Heat Exchanger. *Heliyon* **2020**, *6*, e03401. [CrossRef]
38. Alktranee, M.; Al-Yasiri, Q.; Mohammed, K.S.; et al. Energy, Exergy, and Economic Analysis of Indirect Solar Dryer Integrated Phase Change Material Cans. *Energy Convers. Manag. X* **2025**, *26*, 100986. [CrossRef]
39. Aqib, M.; Shah, M.U.H.; Arbab, M.S.; et al. Energy and Exergy Analysis of Forced Convection Solar Drying of Allium Sativum with and with out Sensible Heat Storage. *MATEC Web Conf*. **2024**, *398*, 01018. [CrossRef]
40. Suherman, S.; Susanto, E.E.; Zardani, A.W.; et al. Energy–Exergy Analysis and Mathematical Modeling of Cassava Starch Drying Using a Hybrid Solar Dryer. *Cogent Eng.* **2020**, *7*, 1771819. [CrossRef]
41. Jeter, S.M. Maximum Conversion Efficiency for the Utilization of Direct Solar Radiation. *Sol. Energy* **1981**, *26*, 231–236. [CrossRef]
42. Malik, A.; Kumar, M. Assessment of a Mixed-Mode Vertical Solar Dryer for Experimental Turmeric Drying. *Sol. Energy* **2024**, *282*, 112980. [CrossRef]
43. Petela, R. Exergy of Heat Radiation. *J. Heat Transf.* **1964**, *86*, 187–192. [CrossRef]
44. Şevik, S.; Aktaş, M.; Dolgun, E.C.; et al. Performance Analysis of Solar and Solar-Infrared Dryer of Mint and Apple Slices Using Energy-Exergy Methodology. *Sol. Energy* **2019**, *180*, 537–549. [CrossRef]
45. Meeso, N.; Nathakaranakule, A.; Madhiyanon, T.; et al. Modelling of Far-Infrared Irradiation in Paddy Drying Process. *J. Food Eng.* **2007**, *78*, 1248–1258. [CrossRef]
46. Bhardwaj, A.K.; Kumar, R.; Kumar, S.; et al. Energy and Exergy Analyses of Drying Medicinal Herb in a Novel Forced Convection Solar Dryer Integrated with SHSM and PCM. *Sustain. Energy Technol. Assess.* **2021**, *45*, 101119. [CrossRef]
47. Aghdam, A.H.; Shaltouki, S.H.; Nikpey, A.H. Comprehensive Evaluation of a Novel Indirect Hybrid Solar Dryer: Conventional and Advanced Exergy Analysis. *Therm. Sci. Eng. Prog.* **2024**, *53*, 102743. [CrossRef]
48. Anuma, O.; Ndukwu, M.C.; Usoh, G.; et al. Energy and Exergy Analysis of a Natural Convection Solar Greenhouse Drier with Insulated Opaque Walls for Drying Aromatic Yellow Pepper. *Renew. Energy* **2024**, *233*, 121141. [CrossRef]
49. Brahma, B.; Shukla, A.K.; Baruah, D.C. Energy, Exergy, Economic and Environmental Analysis of Phase Change Material Based Solar Dryer (PCMSD). *J. Energy Storage* **2024**, *88*, 111490. [CrossRef]
50. Yazici, M.; Kose, R. Energy, Exergy and Economic Investigation of Novel Hybrid Dryer, Indirect Solar Dryer and Traditional Shade Drying. *Therm. Sci. Eng. Prog.* **2023**, *49*, 102502.
51. Daliran, A.; Taki, M.; Marzban, A.; et al. Performance Evaluation of Greenhouse Solar Dryer: Energy-Exergy Analysis, CFD Simulation and Eco-Environmental Assessment. *Renew. Energy* **2025**, *238*, 121946. [CrossRef]
52. Das, B.; Singh, P.; Kalita, P. Sustainable Drying of Baccaurea Ramiflora Using a Mixed-Mode Solar Dryer with Thermal Energy Storage: A Comprehensive 4E Analysis. *Renew. Energy* **2025**, *252*, 123517. [CrossRef]
53. Deepak, C.N.; Behura, A.K. Experimental Analysis of a Mixed Mode Solar Tunnel Dryer for Drying Tomato: Energy, Exergy and Environmental Assessment. *Therm. Sci. Eng. Prog.* **2025**, *63*, 103707. [CrossRef]

54. Kiburi, F.G.; Kanali, C.L.; Kituu, G.M.; et al. Performance Evaluation and Economic Feasibility of a Solar-Biomass Hybrid Greenhouse Dryer for Drying Banana Slices. *Renew. Energy Focus* **2020**, *34*, 60–68. [CrossRef]
55. Heydari, A. Experimental Analysis of Hybrid Dryer Combined with Spiral Solar Air Heater and Auxiliary Heating System: Energy, Exergy and Economic Analysis. *Renew. Energy* **2022**, *198*, 1162–1175. [CrossRef]
56. Abdelkader, T.K.; Sayed, H.A.A.; Refai, M.; et al. Machine Learning, Mathematical Modeling and 4E (Energy, Exergy, Environmental, and Economic) Analysis of an Indirect Solar Dryer for Drying Sweet Potato. *Renew. Energy* **2024**, *227*, 120535. [CrossRef]
57. Singh, A.; Sarkar, J.; Sahoo, R.R. Experimental Performance Analysis of Novel Indirect-Expansion Solar-Infrared Assisted Heat Pump Dryer for Agricultural Products. *Sol. Energy* **2020**, *206*, 907–917. [CrossRef]
58. Bejan, A. *Advanced Engineering Thermodynamics*, 1st ed.; Wiley: Hoboken, NJ, USA, 2016.
59. Dincer, I.; Sahin, A.Z. A New Model for Thermodynamic Analysis of a Drying Process. *Int. J. Heat Mass Transf.* **2004**, *47*, 645–652. [CrossRef]
60. Mugi, V.R.; Chandramohan, V.P. Energy, Exergy, Economic and Environmental (4E) Analysis of Passive and Active-Modes Indirect Type Solar Dryers While Drying Guava Slices. *Sustain. Energy Technol. Assess.* **2022**, *52*, 102250. [CrossRef]
61. Rasheed, L.A.; Yurchenko, A.V.; Mohammed, J.A.-K.; et al. The Effect of Automated Airflow Regulation on the Performance of an Indirect Solar Dryer: A Comparative Study. *Russ. Phys. J.* **2025**, *68*, 288–293. [CrossRef]
62. Hidra, N.; Lehmad, M.; Doubabi, S.; et al. Design and Implementation of an Intelligent Remote Monitoring and Control System for Enhancing Hybrid Solar-Electric Dryer (HSED) Performance. *Dry. Technol.* **2025**, *43*, 1855–1878. [CrossRef]